Feasibility of Contact Elimination of a Mechanical Face Seal Through Clearance Adjustment

Min Zou

Joshua Dayan

Itzhak Green

The George W. Woodruff School of Mechanical Engineering, Georgia Institute of Technology, Atlanta, GA 30332-0405

The feasibility of eliminating contact in a noncontacting flexibly mounted rotor (FMR) mechanical face seal is studied. The approach for contact elimination is based on a parametric study using FMR seal dynamics. Through clearance adjustment it is possible to reduce the maximum normalized relative misalignment between seal faces and, therefore, eliminate seal face contact. Clearance is measured by proximity probes and varied through a pneumatic adjustment mechanism. Contact is determined phenomenologically from pattern recognition of probe signals and their power spectrum densities as well as angular misalignment orbit plots, all calculated and displayed in real-time. The contact elimination strategy is experimentally investigated for various values of stator misalignment and initial rotor misalignment. Contrary to intuition but compliant with the parametric study, the experimental results show that for the seal under consideration contact can be eliminated through clearance reduction. [S0742-4795(00)01503-9]

Introduction

Mechanical face seals are usually used for gas or liquid sealing of rotating shafts. Typical applications can be found in gas turbines, pumps, and compressors. Two types have evolved in mechanical seal design: contacting and noncontacting mechanical face seals. Contacting seals are designed to operate with face contact to minimize leakage at a cost of relatively large friction and wear of the seal faces. Noncontacting seals are designed to operate with certain face separation to reduce frictional heat generation and wear at a cost of some leakage. Statistics of industrial mechanical seals shows that most of them fail prematurely rather than wear out in a normal way [1]. Seal failure comprises a large portion of plant maintenance costs [2]. The state of the art has not proven adequate in guaranteeing noncontacting operation of the most carefully developed mechanical seals, not even for well-defined applications, such as pump seals in the nuclear power industry. Various explanations have been offered to account for unpredictable and premature seal failure, but some basic factors not yet fully understood appear to be the cause. A problem likely to cause seal failure is intermittent contact between the faces. Therefore, contact elimination is of prime importance in preventing seal premature failure, especially in critical applications where seal failure may have severe implications.

Experimental investigation of the dynamics of mechanical seals dates back two decades. Etsion and Burton [3] tested a seal under eccentric loading (i.e., initial stator misalignment) that resulted in ''self-excited oscillations.'' Metcalfe [4] observed seal dynamic whirl at stability threshold to be close to half of the shaft speed in a well-aligned mechanical seal. Sehnal et al. [5] investigated the effects of face coning on the seal performance by comparing torque, face temperature, leakage, and wear of a conventional flat-face seal and of coned face seals. Etsion and Constantinescu [6] found that the stator misalignment and its phase shift are time dependent. Eddy current proximity probes have been the preferred means of measuring the stator motion. All these investigations have been, however, restricted to noncontacting mechanical seals having a flexibly-mounted stator (FMS), where data has been analyzed postmortem in the time domain.

The flexibly mounted rotor (FMR) seal is as prevalent in the industry as the FMS seal. In fact, theoretical work by Green [7,8] has proven that the FMR seal has a superior dynamic behavior compared to the FMS seal. The only experimental investigation available on the dynamic behavior of a FMR seal is that by Lee and Green [9–11]. Results obtained from their test rig showed that the FMR seal was vulnerable to higher harmonic oscillations having superimposed signals of integer multiples of the shaft rotating frequency. Periodic face contact has been determined to be the prime source of such oscillations leading eventually to face wear and imminent failure. After elimination of the higher harmonic oscillations through seal redesign it was found that the deviations between analytical and experimental results did not exceed 15 percent. But, as with all previous experimental investigations, data had been acquired first and analyzed off-line later.

For the purpose of monitoring the seal dynamic behavior in real-time Zou and Green [12] have incorporated a data acquisition system into a personal computer that is capable of acquiring and processing data in real-time by a dedicated on-board processor. They have also introduced the concept of orbit plots for the angular response capable of distinguishing between noncontacting and contacting operation modes. Later, Zou and Green [13] applied a PI control strategy using a personal computer and the same board, not only for data acquisition, but also for control. They have been able to maintain and/or adjust the seal clearance at any desired value, whether fixed or varying. However, the elimination of contact once detected, using clearance adjustment has never been attempted. The purpose of this work is to investigate first analytically and then experimentally whether such a concept is feasible.

Several other studies have dealt with the development of controlled mechanical face seal systems [14–17]. They all concentrated on clearance adjustment through temperature control. Temperatures measured by thermocouples were used as feedback, assuming that these temperatures are directly related to clearance. In reality, the thermocouples measure local temperatures only close to the sealing dam. Adding the likelihood of large thermal inertia, this approach may be vulnerable to large time delays between event occurrence and control action. Obviously, the temperature is also not a direct measure of the clearance; therefore, it may not be the most effective feedback signal for adjusting it.

Seal face contact is usually caused by large relative misalign-

Contributed by the International Gas Turbine Institute (IGTI) of THE AMERICAN SOCIETY OF MECHANICAL ENGINEERS for publication in the ASME JOURNAL OF ENGINEERING FOR GAS TURBINES AND POWER. Paper presented at the International Gas Turbine and Aeroengine Congress and Exhibition, Indianapolis, IN, June 7–10, 1999; ASME Paper 99-GT-147. Manuscript received by IGTI March 9, 1999; final revision received by the ASME Headquarters May 15, 2000. Associate Technical Editor: D. Wisler.

ment between the seal rotor and stator. The study of seal dynamics can help in understanding face noncontacting operation and face separation, and it may suggest a novel strategy of contact control. The present work provides important theoretical insight into the rotordynamics of the noncontacting FMR mechanical face seal utilizing closed-form solutions to assist the strategy of contact elimination. First, the parametric analysis by Zou et al. [18] is applied to the present seal, which affirmatively concludes that contact can be eliminated through variation of the seal clearance. Finally, the feasibility of the proposed contact elimination is investigated experimentally.

Parametric Analysis

Seal Angular Response. The test rig subject for this study is shown in Fig. 1 and is discussed in the next section. The analysis and notation that pertain to the current work are consistent with both the theoretical work of Green [7,8] and the experimental work utilizing the test rig. For conciseness this is not repeated. Only the final results necessary for the current study are summarized below.

In FMR seals the stator misalignment, γ_s, and the initial rotor misalignment, γ_{ri}, always exist due to assembly and manufacturing tolerances, or will eventually develop in time because of shaft deflection and machine deterioration. Both misalignments act as forcing functions to the seal angular modes. The maximum rotor steady-state response to these forcing functions is obtained in terms of static transmissibility, γ_o/γ_s, and dynamic transmissibility, γ_{rI}/γ_{ri}, as follows [7]

$$\frac{\gamma_o}{\gamma_s}=\sqrt{\frac{K_s^2+(D_s\omega)^2}{(K_f+K_s)^2+\left(D_s+\frac{1}{2}D_f\right)^2\omega^2}} \tag{1}$$

$$\frac{\gamma_{rI}}{\gamma_{ri}}=\sqrt{\frac{K_s^2}{[(I_z-I_t)\omega^2+(K_f+K_s)]^2+\left(\frac{1}{2}D_f\omega\right)^2}}, \tag{2}$$

where γ_o is the relative misalignment caused by γ_s only, and γ_{rI} is the relative misalignment caused by γ_{ri} only. K_f and D_f are the fluid film angular stiffness and damping coefficients, respectively [19]. K_s and D_s are the rotor support angular stiffness and damping coefficients, respectively [10]. I_z and I_t are the rotor polar and transverse moment of inertia, and ω is the shaft speed.

Assuming that superposition is valid for small perturbations about the working point (the nominal design point at steady-state), the maximum total relative misalignment between the rotor and stator, $\gamma_{\max}$, is the sum of the rotor responses to both the stator misalignment and the initial rotor misalignment:

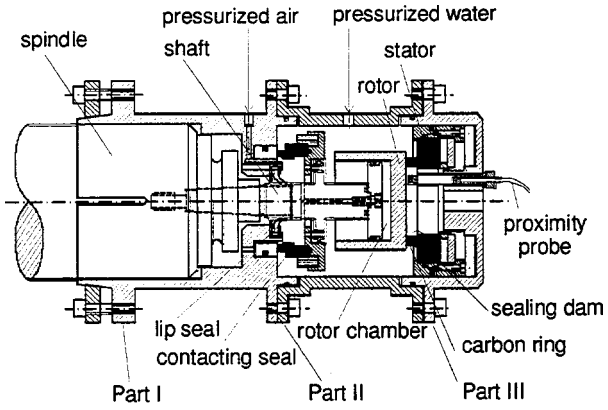

Fig. 1 Schematic of the FMR noncontacting mechanical seal assembly

$$\gamma_{\max}=\gamma_o+\gamma_{rI}. \tag{3}$$

When this relative misalignment is too large it will cause face contact. A basic requirement to avoid contact from the onset is to ensure hydrostatic stability via positive angular film stiffness [19]. In which case, a properly designed seal must have a normalized coning angle, $\beta^*=\beta r_o/C_o$, that is greater than the critical value, $\beta^*_{\text{critical}}=1/R_i$ (where $R_i=r_i/r_o$ is the dimensionless inner radius). Should face contact still occur because of a large dynamic angular response, it will take place at the minimum film thickness at the inner radius. Mathematically, contact is determined whenever the maximum relative misalignment between the seal faces, $\gamma_{\max}$, exceeds a critical value. In a normalized form this condition is [7]:

$$\gamma^*_{\max}=\frac{\gamma r_o}{C_o}>\gamma^*_{\text{critical}}=\frac{1}{R_i}, \tag{4}$$

where r_o is the seal outside radius, and C_o is the clearance. Thus, seal design, manufacturing and operation should ensure $\gamma^*_{\max}<\gamma^*_{\text{critical}}$ at all times in order to avoid face contact.

Parameter Effects. In most applications, the operating conditions of the mechanical seal are not precisely known. Disturbances and variations of operating conditions and the lack of adjustment mechanism to counteract them may cause face contact, ultimately leading to face wear and seal failure. Thus, the incorporation of an active control mechanism may reduce the danger of failure and increase seal reliability. Studying the effects of different input variables on the total normalized relative misalignment may suggest possible control parameters for a contact elimination strategy.

The parameters of Eqs. (1)–(3) are affected by two kinds of basic physical variables: seal geometry, e.g., seal inside and outside diameters and conning angle; and operational variables, such as sealed fluid (lubricant) viscosity, sealed pressure, shaft speed, and clearance. The results of this research are applied to the seal test rig (Fig. 1) with fixed seal size and sealed pressurized water. In particular, the effects of two parameters are actually tested on the rig and are presented here. The first is the clearance—an operating variable, which has been sought as the variable to be adjusted. The second is the seal coning angle—a geometrical variable that always exists in practical mechanical seals, which strongly affects the rotordynamic coefficients and, therefore, the clearance. The effects of other parameters have been studied elsewhere [18].

In Fig. 2 the maximum normalized relative misalignment, $\gamma^*_{\max}$, is plotted as a function of the coning angle for several clearances at different sealed water pressures and shaft speeds. In order to avoid seal face contact it is necessary that the maximum normalized relative misalignment should always be less than $\gamma^*_{\text{critical}}$. In the present application $\gamma^*_{\text{critical}}$ is 1.25 (shown as a bold horizontal line), such that $\gamma^*_{\max}$ less than 1.25 indicates noncontacting operation, while any $\gamma^*_{\max}$ greater than 1.25 indicates face contact.

At a given shaft speed of 80 rad/s, Fig. 2(*a*) shows that when the sealed water pressure is relatively small (100 kPa), noncontacting operation can be attained only for a seal having small coning angles (<0.7 mrad) and small clearances (<2 μ). Fig. 2(*b*) shows that at the said speed noncontacting operation is possible at larger coning angles (2–10 mrad), but only at larger clearances (>4 μ) and only if the sealed water pressure is increased to 900 kPa. As shown in Figs. 2(*c*) and 2(*d*), higher shaft speeds contribute to widening of the ranges for viable coning and clearance, and it is attributed to an amplified aligning gyroscopic effect. For example, at low sealed pressure (100 kPa) but high shaft speed (360 rad/s) a seal having a coning angle of almost 2 mrad can be maintained in noncontacting mode of operation provided the clearance is smaller than 2μ. Similarly, at a high pressure (900 kPa) and a high speed (360 rad/s) a seal having coning angles in the range of 1–10 mrad can be maintained in noncontacting mode of operation provided that the clearance is 4 μ or larger. Gener-

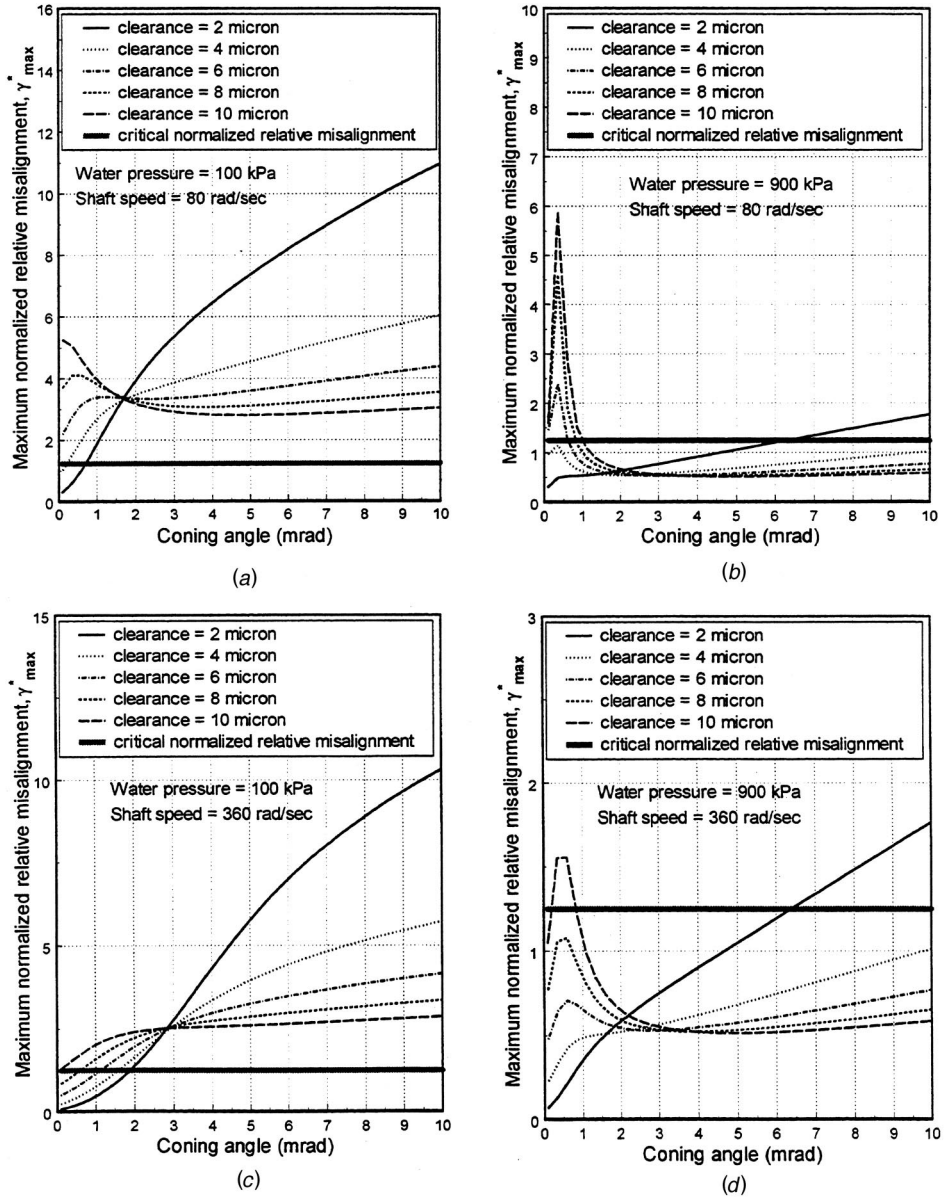

Fig. 2 Maximum normalized relative misalignment—coning angle relationship

ally, seals operating at small clearances and relatively small coning angles are preferred because they assume larger fluid film stiffness and damping, and yield smaller leakage. Operating seals with small coning angles and large clearances, or seals having large coning angles and small clearances should be avoided because they leak more and are more prone to contact.

Examination of all four cases presented in Fig. 2 reveals that if the seal under investigation possesses coning angles smaller than 1.5 mrad, then reducing the clearance invariably reduces the maximum normalized relative misalignment, and with it the likelihood of contact. And vise versa for large coning angle (>3 mrad), where reducing the clearance increases the maximum normalized relative misalignment.

This parametric analysis has been instrumental in establishing that small clearances and small coning angles are preferred for the safer operation of the current seal. As in any commercial application the current seal faces have been lapped to a flatness of about 1 μm maximum peak to valley height. Seal coning, however, is the outcome of various deformations caused by the hydraulic (sealed) pressure, centrifugal effects, and interface (sealing dam) heating. These effects are normally coupled and, therefore, in reality the coning is uncontrollable over a sustained period of time. The present study indicates, however, that in the current seal it is sufficient for the coning to fall into the range of ''small coning angles'' to allow for face contact to be eliminated via clearance adjustment (in this case, clearance reduction). From a controllability point of view, it was found [20] that the maximum normalized relative misalignment is most sensitive to clearance changes at a coning angle of about 0.5 mrad, or at coning angles that are greater than 3 mrad. At these coning angles the control effort is minimized. The best control results can be achieved, however, at the smallest coning angle, i.e., the critical coning angle needed for positive fluid film stiffness [19]. The critical coning angle varies with the clearance, and for the tested seal it ranges from 0.0984 mrad to 0.492 mrad for clearances of 2 μm to 10 μm, respectively.

As mentioned, stator and initial rotor misalignments are responsible for γ_{max}. The parametric study performed above (that is based on a linearized analysis with the assumption of ''small perturbations'' about equilibrium) is very valuable for seal design

and performance prediction. It can also provide guidelines for action should contact occur. But other factors, such as uncertainties about the kinematics of the flexible support and its rotordynamic coefficients, machine deterioration, transients in sealed pressure or shaft speed, or unexpected shaft vibration, will all affect the dynamic behavior of the seal and, hence, the relative position between rotor and stator. This is where strict reliance on precise analysis loses effectiveness because some or all of the assumptions imbedded in the analysis may be borne out physically. Particularly, when intermittent face contact occurs the assumption and analysis of a ''noncontacting'' seal become irrelevant. The only analysis of intermittent seal face contact has been performed by Lee and Green [9] who observed higher harmonic oscillations (HHO), and offered a contact model based on a Fourier series expansion. Therefore, when it comes to actual diagnostics a phenomenological approach for contact detection is more appropriate, and indeed such an approach is adopted here.

Contact Elimination

Seal Test Rig. The noncontacting FMR mechanical face seal test rig used in this study (Fig. 1) is essentially identical to that in Lee and Green [9–11], equipped, however, with the more advanced real-time data acquisition and analysis system introduced by Zou and Green [12,13]. Other significant modifications include now the stator, which is made entirely of carbon graphite, and the rotor, which is made entirely of AISI 440C stainless steel. Both have been fabricated and lapped to industry standards by seal manufacturers. All these modifications facilitate more reliable measurement and determination of the relative position between rotor and stator.

The rotor is flexibly mounted on the rotating shaft through an elastomer O-ring. This allows the rotor to track the stator misalignment and to move axially. The seal stator assembly is composed of several components: the carbon stator, the spacer, and the stator holders. This design is capable of mechanically deforming the stator and produces seals with different coning angles [10]. For stability it is mandatory for the seal to maintain a converging gap in the direction of radial flow. For an outside pressurized seal the minimum seal film thickness has to be on the ID [19]. Transients in deformations caused by thermal effects, for example, occur at much slower pace than the time scale of interest in seal dynamics. Therefore, the two processes can be regarded as decoupled. For this reason the coning in the present test rig is induced by deforming the faces in the stator fixture and held fixed throughout the experiments. In that regard, data sufficient for dynamic analysis and monitoring is acquired in a fraction of a second, a time scale insignificant for any thermal deformations to occur. Moreover, as mentioned contact is detected here on a phenomenological basis, so it is not necessary to know where contact occurs; all that matters is that it occurs somewhere.

The stator assembly is fixed in the housing, which is made of three parts for convenience in machining, maintenance, and adjustment of the test rig. All possible leakage paths are sealed by O-rings. The sealed fluid in the housing is pressurized water. The shaft is connected to a spindle driven by a DC motor through two timing pulleys and a timing belt. A speed controller controls the motor speed.

Pressurized air is supplied from the main air supply line to the rotor chamber through holes in the housing and the shaft. It is sealed by a lip seal at one end and separated from the water by a contacting seal at the other end. The seal operates at an equilibrium clearance where the opening and closing forces are balanced. Changing the closing force by adjusting the air pressure in the rotor chamber (whether manually or by the computer through a voltage to pressure converter) varies the clearance. Further details of the test rig components, data acquisition and analysis can be found in the aforementioned references.

Clearance Adjustment. Three eddy current proximity probes mounted on the end of the housing measure the instantaneous dynamic response of the rotor along the shaft axis. These proximity probes have a bandwidth of about 10 kHz. They can measure the static and dynamic distances between their tips and the rotor face end surface. Key parameters including stator misalignment, rotor misalignment, relative misalignment between the rotor and the stator are calculated on-line in real-time from the probe measurements [12]. The clearance of the seal is obtained as follows: when the shaft is stationary, high air pressure is applied in the rotor chamber to ensure that the rotor is pressed against the stator, at which state the probe readings are taken. The average readings of the two probes mounted 180 deg apart represents the reference for zero clearance. The clearance of the seal at any time is then the difference between the instantaneous average readings of these two probes and the zero reference. (Sehnal et al. [5], and Etsion and Constantinescu [6], have made similar attempts to determine the clearance from proximity probe readings, but they reverted to indirectly estimating the clearance from a simplified equation applied to the measured leakage.) A low pass filter with a cut-off frequency of 1 kHz is used to eliminate high frequency cross-talk noise among the probes and also to serve as an anti-aliasing filter. The proximity probe signals in terms of the reduced voltages are sent through the A/D converters to a floating-point Digital Signal Processor (DSP). This DSP, supplemented by a set of on-board peripherals, such as analog to digital (A/D) and digital to analog (D/A) converters, comprise a universal board mounted in a personal computer. The seal clearance is then calculated and compared with the desired value. Based on the error signal between the measured clearance and the desired one a control signal is sent to the electropneumatic transducer (through the D/A converter), which provides a proportional air pressure signal. Zou and Green [13] provided an in-depth description and implementation of the said control scheme.

Experimental Results. The feasibility of contact elimination through clearance adjustment is now experimentally investigated. The proximity probe measurements are used as feedback to calculate the clearance. The experiments are conducted at 344.8 kPa water pressure and 28 Hz (176 rad/s) shaft speed, i.e., well within the range investigated in Fig. 2. The coning angle is set to 1 mrad, roughly twice as large as the largest critical value and sufficiently close to the optimal value of 0.5 mrad for minimum effort control (see above). Two sets of experiments are presented. Fig. 3 to Fig. 5 show the results for experiments with small stator initial rotor misalignments, both of 0.5 mrad, and Fig. 6 to Fig. 8 for experi-

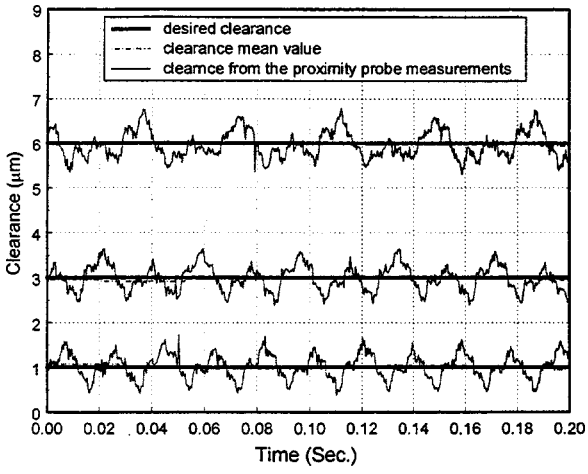

Fig. 3 Desired clearances and clearances calculated from proximity probe measurements (small stator and initial rotor misalignments $\gamma_s = \gamma_{ri} = 0.5$ mrad)

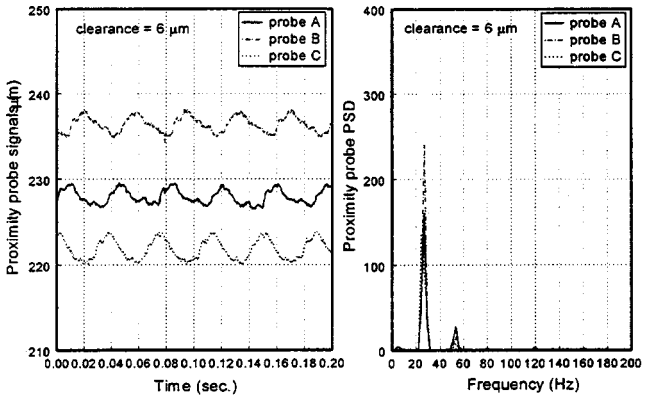

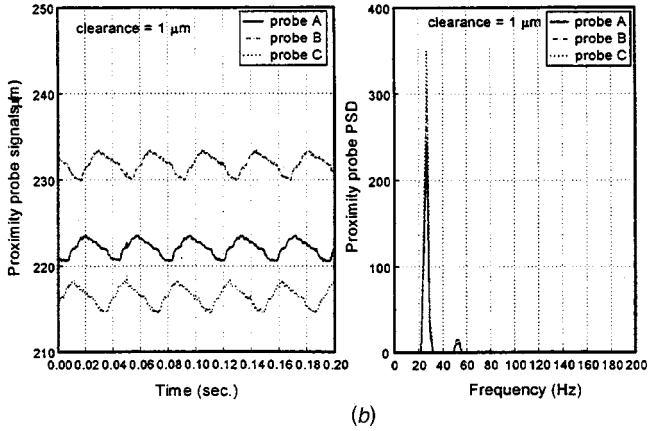

Fig. 4 Proximity probe signals and their PSDs for different clearances (6 μm and 1 μm) (small stator and initial rotor misalignments $\gamma_s = \gamma_{ri} = 0.5$ mrad)

mental results with large stator and initial rotor misalignments, both of 1.5 mrad. Other experiments for mixed misalignments [21] show similar behavior.

The desired clearance is stepwise set to 6 μm, 5 μm, 4 μm, 3 μm, 2 μm, and 1 μm, and held constant by a PI controller [13], to investigate one at a time the clearance effect on seal face contact. Figures 3 and 6 show the desired clearances, the actual clearances

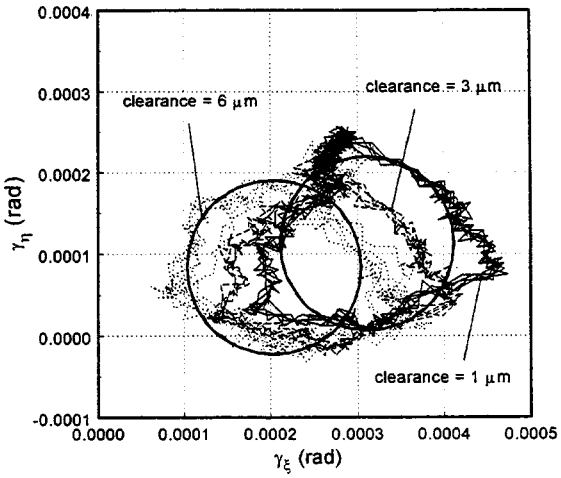

Fig. 5 Rotor angular misalignment orbit for different clearances (6 μm, 3 μm, and 1 μm) (small stator and initial rotor misalignments $\gamma_s = \gamma_{ri} = 0.5$ mrad)

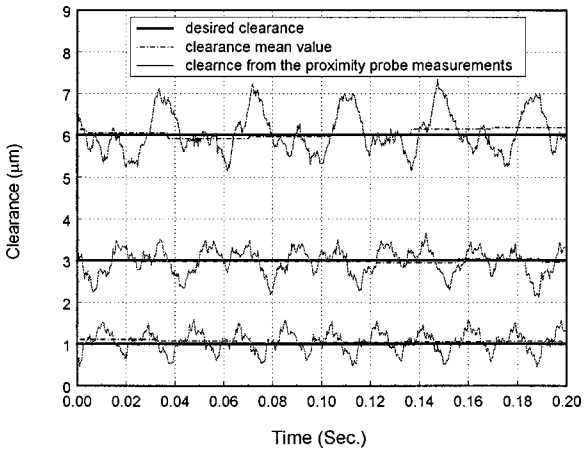

Fig. 6 Desired clearances and clearances calculated from proximity probe measurements (large stator and initial rotor misalignments $\gamma_s = \gamma_{ri} = 1.5$ mrad)

calculated from the measurements of the two proximity probes mounted 180 deg apart, and the calculated clearance mean value for each revolution (for clarity the graphs depict results for 6, 3, and 1 μm only). Unlike the theoretical assumption of constant clearance, the measured clearance is periodic and contains higher harmonic oscillations (HHO). The peak to peak value of the mea-

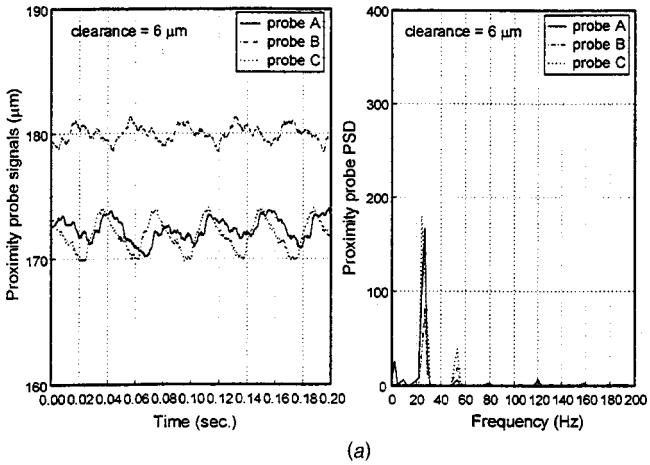

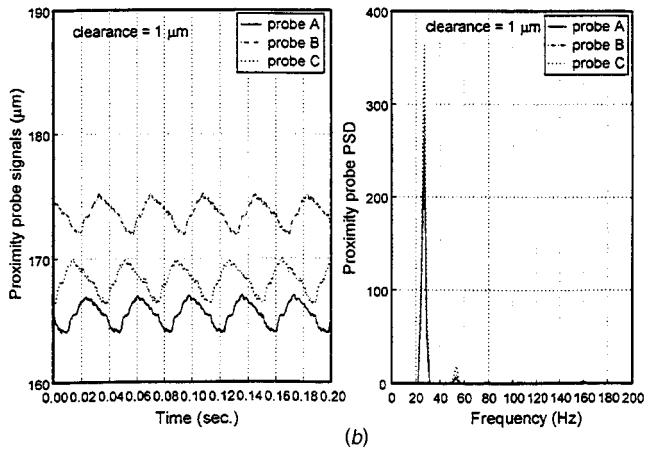

Fig. 7 Proximity probe signals and their PSDs for different clearances (6 μm and 1 μm) (large stator and initial rotor misalignments $\gamma_s = \gamma_{ri} = 1.5$ mrad)

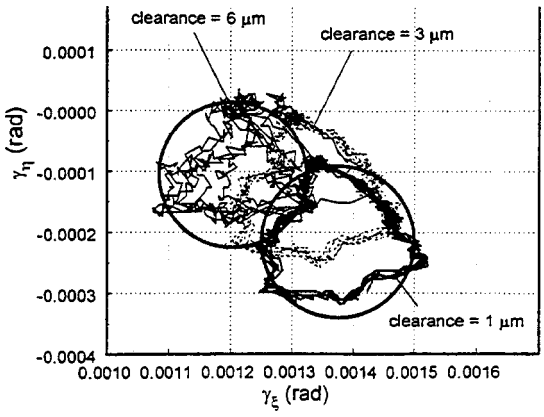

Fig. 8 Rotor angular misalignment orbit for different clearances (large stator and initial rotor misalignments $\gamma_s = \gamma_{ri} = 1.5$ mrad)

sured clearance decreases and there are less HHO present in the measured clearance signal as the clearance is reduced.

Because of the factors mentioned above and because the measured clearance oscillates, face contact is not determined based on the theoretical (or calculated) normalized relative misalignment. Instead, it is based on the pattern of the three probe signals and their power spectrum densities (PSD). Figures 4 and 7 show the three proximity probe signals and their associated power spectrum densities for desired clearances of 6 μm, and 1 μm, respectively. (The plots for all intermediate values show similar behavior, see Zou [21].) The PSD for all clearances have second higher harmonic oscillations (HHO), which are equal to twice the shaft rotating frequency. Certain levels of these HHO are inherent in the system. They are present even when the rotor runs without the stator in place. Other system components, particularly the O-ring flexible support, are suspected to induce these second HHO. It should be noted, however, that their energy level at the largest clearance case (6 μm) is much higher than that at the smallest clearance case (1 μm). Indeed, it is clearly visible (Figs. 4(*a*), and 7(*a*)) that when the clearance is large (6 μm), the shape and the peak to peak value of each probe signal is different from the others and is accompanied by the above mentioned pronounced HHO. As seal clearances decrease the shape and peak to peak value of the probe signals change as well, and tend to become similar to each other. When clearance reaches 1 μm the three probe signals are almost identical, where HHO have practically disappeared. It can also be noticed that in the largest clearance, Figs. 4(*a*) and 7(*a*) contain sub harmonics and super high harmonics. However, as the seal clearance decreases (particularly to 1 μm—see Figs. 4(*b*) and 7(*b*)), the sub and super higher harmonics have vanished. The absence of HHO in the PSD is an indication that noncontacting operation has been restored (see [9]).

The angular response orbit [12] is used as another means of diagnostics that capture the rotor angular dynamic behavior. It represents the locus of the magnitude of the rotor misalignment vector positioned at the instantaneous precession angle. Figures 5 and 8 show the rotor angular misalignment orbit for the desired clearances of 6 μm, 3 μm, and 1 μm. (The results of 5 μm, 4 μm, and 2 μm, are similar and were omitted for clarity.) Two circles are drawn in Figures 5 and 8 through orbit data obtained for the 6 μm clearance and for the 1 μm clearance (no circle is drawn through the 3 μm data because it is very similar to the 1 μm case). It is readily seen that the deviation of the data from a perfect circle in the 6 μm case is far bigger than that of the 1 μm cases. An odd shape cluster of data points in the 6 μm case of Fig. 5 (the blackened area shown at the top of the postulated circles), denotes part of the 6 μm orbit which clearly does not belong to the circle. Indeed, the orbit shape becomes more circular as the clearance decreases, which is another indication of noncontacting operation [12]. Therefore, the absence of high harmonics in the PSD plot for these data and the more circular orbits obtained for decreased clearance both show that contact can indeed be eliminated by such clearance adjustment. In summary, using the proximity probes' measurements as feedback in a straightforward control loop, interpreting the existence of high harmonics or non-circular orbits as contact, and applying the necessary closing force on the FMR to adjust the clearance, eliminates that contact. As mentioned, additional experimental results for the mixed cases of large stator misalignment with small initial rotor misalignment and vise versa also support these findings.

Conclusions

This research suggests that contact elimination may be achieved through clearance adjustment. The feasibility of doing so is experimentally investigated using FMR seal dynamics with large and small stator and rotor misalignments. Contact detection and elimination is demonstrated for two combinations of stator misalignments and initial rotor misalignment when both are 0.5 mrad, and then when both are 1.5 mrad. The clearance is calculated in real-time from the measurements of proximity probes and is varied through a pneumatic closing force adjusting mechanism in the test rig. All experimental results show that contact can be eliminated through clearance adjustment. Moreover, these experimental results are predicted by the parametric study. Particularly for the tested seal and contrary to intuition, it is found that the maximum normalized relative misalignment decreases with the clearance and, therefore, the likelihood of face contact decreases as well. Therefore, once seal contact is detected by the phenomena described (i.e., HHO detected by PSD and/or noncircular orbit plots), it can be eliminated by adjusting the clearance to a smaller value.

Worthy of notice is that most previous research on controlled mechanical seals used temperature control instead of clearance control. When the seal clearance reduces, the temperature at the sealing dam may rise because of increased viscous heating. In such a case, the action that would be taken by a controlled system relying on temperature would be to increase the clearance. This, contrary to the finding of this research, is likely to have detrimental consequences on the seal.

Likewise it must be highlighted that the clearance cannot be decreased just without bounds. Clearly if the clearance is decreased to the point where surface asperities start rubbing, the basic assumption of ideal noncontacting operation ceases to be accurate. The goal in seal design, and now in seal monitoring and control, is to maintain the smallest clearance possible with either minimal face contact or no face contact at all. It is believed that the technology developed in this research can assist in accomplishing this goal.

Advancing this technology in real practice is to automate the two processes of contact detection, and then contact elimination. This consequently will necessitate the development of a strategy for automatic clearance adjustment to a new desired value, which may be based upon a certain measure of the variations of PSD and/or orbit plots from a known or ideal noncontacting behavior.

Acknowledgments

The authors wish to express their appreciation to the Office of Naval Research for support of research grant N00014-95-1-0539, entitled *Integrated Diagnostics*. Dr. Peter Schmidt serves as program officer. The authors also wish to express their appreciation to Mr. Andrew Flaherty and Rexnord Corporation for machining the seal rotor, to Mr. Laurence Thorwart and Mr. David Erich of Pure Carbon Company for providing the carbon seals used in this study. This project is also supported in part by a Georgia Tech foundation Grant, E25-A77, made by Mr. Gilbert Bachman. This support is gratefully acknowledged.

References

[1] Buck, Jr., G. S., 1980, ''A Methodology for Design and Application of Mechanical Seals,'' ASLE Trans., **23**, No. 3, pp. 24–252.

[2] Will, Jr., T. P., 1982, ''Experimental Observation of a Face-Contact Mechanical Shaft Seal Operation on Water,'' Lubr. Eng., **38**, No. 12, pp. 767–772.

[3] Etsion, I., and Burton, R. A., 1979, ''Observation of Self-Excited Wobble in Face Seals,'' ASME J. Lubr. Technol., **101**, No. 4, pp. 526–528.

[4] Metcalfe, R., 1982, ''Dynamic Whirl in Well-Aligned, Liquid-Lubricated End-Face Seals with Hydrostatic Tilt Instability,'' ASLE Trans., **25**, No. 1, pp. 1–6.

[5] Sehnal, J., Sedy, J., Zobens, A., and Etsion, I., 1983, ''Performance of the Coned-Face End Seal with Regard to Energy Conservation,'' ASLE Trans., **26**, No. 4, pp. 415–429.

[6] Etsion, I., and Constantinescu, I., 1984, ''Experimental Observation of the Dynamic Behavior of Noncontacting Conedface Mechanical Seals,'' ASLE Trans., **27**, No. 3, pp. 263–270.

[7] Green, I., 1989, ''Gyroscopic and Support Effects on the Steady-State Response of a Noncontacting Flexibly-Mounted Rotor Mechanical face Seal,'' ASME J. Tribol., **111**, pp. 200–208.

[8] Green, I., 1990, ''Gyroscopic and Damping Effects on the Stability of a Noncontacting Flexibly-Mounted Rotor Mechanical Face Seal,'' *Dynamics of Rotating Machinery*, Hemisphere Publishing, Bristol, PA, pp. 153–173.

[9] Lee, A. S., and Green, I., 1994, ''Higher Harmonic Oscillation in a Flexibly Mounted Rotor Mechanical Seal Test Rig,'' ASME J. Vibr. Acoust., **116**, No. 2, pp. 161–167.

[10] Lee, A. S., and Green, I., 1995, ''Physical Modeling and Data Analysis of the Dynamic Response of Flexibly Mounted Rotor Mechanical Seal,'' ASME J. Tribol., **117**, No. 1, pp. 130–135.

[11] Lee, A. S., and Green, I., 1995, ''An Experimental Investigation of the Steady-State Response of a Noncontacting Flexibly Mounted Rotor Mechanical Face Seal,'' Trans. ASME, J. Tribol., **177**, No. 1, pp. 153–159.

[12] Zou, M., and Green, I., 1997, ''Real-Time Condition Monitoring of Mechanical Face Seal,'' *Proceedings the 24th Leeds-Lyon Symposium on Tribology*, London, Imperial College, pp. 423–430.

[13] Zou, M., and Green, I., 1999, ''Clearance Control of a Mechanical Face Seal,'' STLE Tribol. Trans., **42**, No. 3, pp. 535–540.

[14] Salant, R. F., Miller, A. L., Kay, P. L., Kozlowski, J., Kay, W. E., and Algrain, M. C., 1987, ''Development of an Electrically Controlled Mechanical Seal,'' *Proceedings 11th International Conference on Fluid Sealing*, BHRA, pp. 576–595.

[15] Heilala, A. J., and Kangasneimi, A., 1987, ''Adjustment and Control of a Mechanical Seal Against Dry Running and Severe Wear,'' *Proceedings 11th International Conference on Fluid Sealing*, BHRA, pp. 548–575.

[16] Etsion, I., Palmor, Z. J., and Harari, N., 1991, ''Feasibility Study of a Controlled Mechanical Seal,'' Lubr. Eng., **47**, No. 8, pp. 621–625.

[17] Wolff, P., and Salant, R. F., 1995, ''Electronically Controlled Mechanical Seal for Aerospace Applications: Part II—Transient Tests,'' Tribol. Trans., **38**, No. 1, pp. 51–56.

[18] Zou, M., Dayan, J., and Green, I., 1999, ''Parametric Analysis for Contact Control of a Noncontacting Mechanical Face Seal,'' *Proceedings of Vibration, Noise & Structural Dynamics*, Venice Italy, April 28–30, 1999, pp. 493–499.

[19] Green, I., 1987, ''The Rotor Dynamic Coefficients of Coned-Face Mechanical Seals with Inward or Outward Flow,'' ASME J. Tribol., **109**, No. 1, pp. 129–135.

[20] Dayan, J., Zou, M., and Green, I., 1999, ''Sensitivity Analysis for the Design and Operation of a Noncontacting Mechanical Face Seal,'' J. Mech. Eng. Sci., in print.

[21] Zou, M., 1998, ''Real-Time Monitoring and Control of a Noncontacting Mechanical Face Seal,'' Ph.D. thesis, Georgia Institute of Technology, Atlanta, GA.